Inverse melting in the Ti-Cr system

Z. H. Yan,* T. Klassen, C. Michaelsen, M. Oehring, and R. Bormann
Institute for Materials Research, GKSS-Research Center, D-2054 Geesthacht, Germany
(Received 16 June 1992; revised manuscript received 19 January 1993)

Investigations of metastable phase transformations demonstrate that a polymorphous transformation from a crystal to a glass, the so-called inverse melting, is possible in the Ti-Cr system, however at different Cr concentrations compared to earlier reports. Single-phase, metastable bcc β-TiCr alloys with Cr concentrations between 40 and 65 at. % are prepared by mechanical alloying. A subsequent heat treatment results in a transformation into an amorphous phase. Complete amorphization is observed only in a narrow range around 55 at. % Cr, while two-phase equilibria between the bcc and the amorphous phase are found for other compositions. The experiments are in good agreement with the metastable phase diagram which is obtained from the free energy curves determined by the calculation-of-phase-diagram (CALPHAD) method.

I. INTRODUCTION

In recent years a variety of methods have been developed to synthesize amorphous alloys by solid-state reactions,[1] e.g., by interdiffusion of multilayers,[2] by mechanical alloying of elemental powders,[3] and by annealing crystalline compounds that are only stable at higher pressures.[4] The formation of an amorphous phase in these processes can be understood from the thermodynamics of the particular system, which provides a driving force for the amorphization reaction.[1] However, the formation of the equilibrium phases has to be kinetically suppressed, which can be expected only for the early stages of phase reactions or under conditions where the stable phases are energetically destabilized.

In addition, vitrification of a high-temperature phase has been claimed,[5,6] which is quite unexpected from a thermodynamic point of view[7,8] as it requires a lower entropy for the amorphous phase than for the crystalline state. Metastable bcc β-TiCr phases with Cr contents between 30 and 40 at. % were prepared by laser irradiation[5] or by quenching from high temperatures[6] and were subsequently annealed at 600 °C, resulting in an amorphization. This transition was named "spontaneous vitrification" or "inverse melting," in the case where a polymorphous transformation occurs. Furthermore, it was reported that the transition is reversible, such that the alloy can be switched back and forth between the amorphous and the bcc crystalline phase by application of alternating annealing steps at 800 and 600 °C.[5]

While several research groups have investigated this topic, with the exception of one report,[9] none of them were able to reproduce the transformation into the amorphous state.[10,11] As the experimental evidence for the amorphization is not completely convincing, the question arises as to whether inverse melting is in principle possible in this system. Therefore, some groups have tried to assess, on the basis of thermodynamics, whether there is a driving force in free energy for inverse melting, leading to a negative result in some cases.[7,12,13] However, it should be noted that thermodynamic analyses depend critically on models and assumptions, especially in the Ti-Cr system where the free-energy differences between the amorphous and the bcc phases might be small.

This paper reports a systematic investigation on inverse melting of bcc-TiCr alloys with Cr contents ranging from 40 to 65 at. %. The work is focused on the influence of concentration and annealing conditions on the amorphization reaction, with the aim of studying the kinetic process as well as the underlying thermodynamics. The metastable β-TiCr alloys are prepared by mechanical alloying of elemental powder blends. Other preparation techniques, such as quenching of bcc alloys from high temperatures, usually fail to produce homogeneous bcc phases, in particular at higher Cr contents, as the nucleation of the stable phases, e.g., $TiCr_2$, cannot be kinetically suppressed completely. In the case of mechanical alloying, intermetallic compounds are energetically destabilized during milling,[14] thus allowing the preparation of the metastable bcc phase.

The results of the phase transformation are discussed using the free-energy curves of the Ti-Cr system calculated by the CALPHAD method.[15] The advantage of the CALPHAD approach originates from the possibility to critically assess the consistency of experimental thermodynamic data, and to calculate thermodynamic functions which can be extrapolated into a metastable composition or temperature range.[16,17]

II. EXPERIMENTAL

A planetary ball mill (Fritsch Pulverisette 5) with hardened steel vials and balls was employed for mechanical alloying. All handling of the powders including the milling procedure was performed in a glove box, in which the Ar atmosphere was continuously purified, in order to keep its oxygen and water content below 1 ppm. Elemental Ti (99.8%) and Cr (99.8%) powder blends with particle sizes smaller than 300 μm were prepared in the composition range from 40 to 65 at. % Cr in steps of 5 at. %. The gaseous impurity content of $Ti_{60}Cr_{40}$ powders, milled for 150 h, was determined by chemical analysis to be

0.0084 wt % H and 0.20 wt % O, which is comparable to the impurity level of the elemental powder components. The Fe contamination of all alloyed powders investigated amounts to less than 2.2 wt %, and results mainly from abrasion of the vials and balls used for the milling. The structural evolution during mechanical alloying and subsequent annealing was characterized by x-ray-diffraction (XRD) analysis using Cu-K_α radiation.

The heat treatment of as-milled alloys was carried out using a Perkin Elmer differential scanning calorimeter (DSC-2). The specimens were heated in Cu pans under purified Ar (99.9999%) flow. Prior to the experiment, the air was carefully removed from the DSC cell by pumping and flushing with Ar several times in order to avoid any oxygen influence on the occurring phase transformations. In addition, DSC measurements were carried out in a high-temperature calorimeter of type Netzsch DSC 404 using 99.999% Ar.[18] As for the measurements with the DSC-2, care was taken to remove the air from the furnace prior to the DSC runs. For transmission electron microscopy (TEM) a Philips 400 T was used operating at 120 kV. TEM specimens were prepared by cold pressing a mixture of sample and aluminum powders and jet-polishing the compacts with an electrolyte consisting of 430 ml methanol, 250 ml butanol, and 18 ml perchloric acid, 70%.[19]

III. RESULTS

A. Mechanical alloying of Ti-Cr

The structural evolution, upon milling of $Ti_{60}Cr_{40}$ elemental powder blend, is shown in Fig. 1, as a function of milling time. After 10 h additional diffraction peaks occur corresponding to a Ti-rich bcc phase. The hcp Ti completely disappears after 50 h of milling, and a mixture of two bcc phases with different compositions coexist. Upon further milling the alloy homogenizes, leading to a bcc $Ti_{60}Cr_{40}$ alloy with a lattice constant of 0.312 nm. However, it is noted that even after 150 h of milling some residual traces of unalloyed Cr can be detected from the x-ray analysis. The bcc alloy exhibits a very broad diffraction pattern resulting from a reduced grain size and from internal strain of the lattice. By applying the method developed by Williamson and Hall[20] and described in detail in Ref. 21 an average crystallite size of 34 nm and a root-mean-square (rms) strain $\langle \epsilon^2 \rangle^{1/2}$ of 1.6% are determined.

Figure 2 shows the XRD patterns of the final products after a milling time of 150 h as a function of Cr content. The elemental powder blends react to form homogeneous β-TiCr phases, indicating that mechanical alloying is a suitable approach for preparing metastable bcc TiCr alloys over the entire compositional range. The lattice constants of the bcc structures are plotted in Fig. 3 versus the Cr content, including the values for pure bcc Cr and Ti. The concentration dependence of the lattice constant is in good agreement with available data from the literature,[22] and can be described by Vegard's law proposing a linear interpolation between the lattice constants of the pure components. This suggests that defects in the as-milled state do not influence the lattice spacing. The results can be fitted by the following linear equation:

$$a = 0.328 \text{ nm} - 0.0398 \text{ nm} \cdot x_{\text{Cr}} , \quad (1)$$

where a is the lattice constant in nm, and x_{Cr} the molar

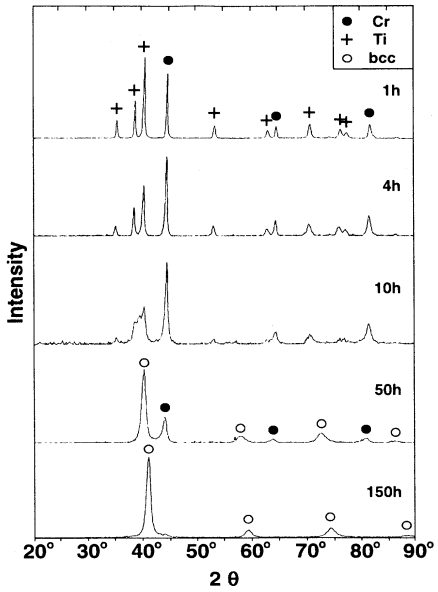

FIG. 1. X-ray-diffraction patterns obtained with Cu-K_α radiation from mechanically alloyed $Ti_{60}Cr_{40}$ after selected milling times.

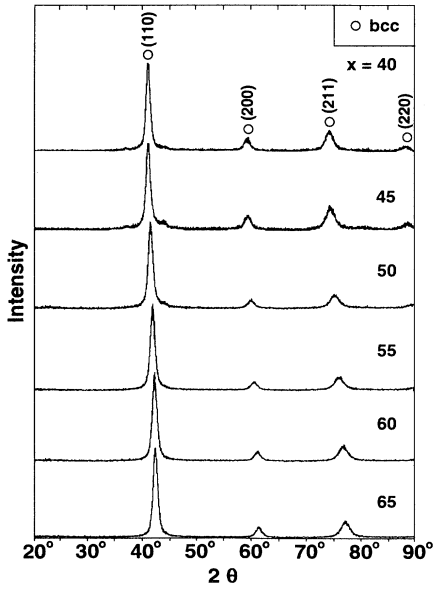

FIG. 2. X-ray-diffraction patterns from the final products of mechanically alloying of $Ti_{100-x}Cr_x$ powder blends, for different Cr concentrations.

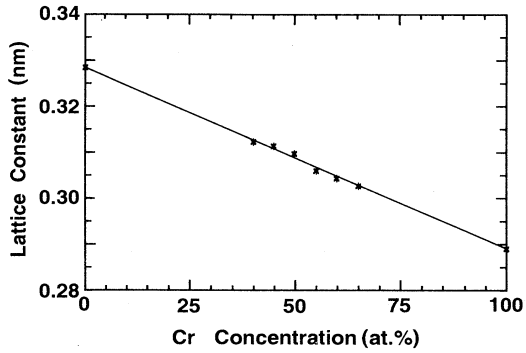

FIG. 3. Lattice parameter of the mechanically alloyed bcc alloys vs Cr content.

fraction of Cr. Equation (1) may be used to determine the composition of the bcc phase from its lattice constant.

B. Heat treatment of mechanically alloyed $Ti_{60}Cr_{40}$ samples

β-$Ti_{60}Cr_{40}$, prepared by laser irradiation or by water quenching of the bcc alloy, was reported to undergo amorphization,[5,6] and therefore most subsequent investigations[9–13,23] were focused on this composition. The annealing behavior of bcc $Ti_{60}Cr_{40}$ prepared by mechanical alloying has been investigated by means of DSC, in combination with subsequent x-ray-diffraction analyses after rapid cooling with a rate of 320 K/min. Figure 4 shows a DSC scan, which exhibits three exothermal peaks at approximately 400, 580, and 680 °C respectively. In order to study the corresponding phase transitions, the samples were heated up to temperatures labeled as *A* (after the first DSC peak), *B* (within the second peak), *C* (after the second peak), and *D* (after the third peak) in Fig. 4, and then quenched. The corresponding XRD results are shown in Fig. 5, including the diffraction pattern obtained before annealing for comparison. After heating over the first broad exothermal peak *A*, the diffraction peaks sharpen, reflecting some structural relaxation or re-

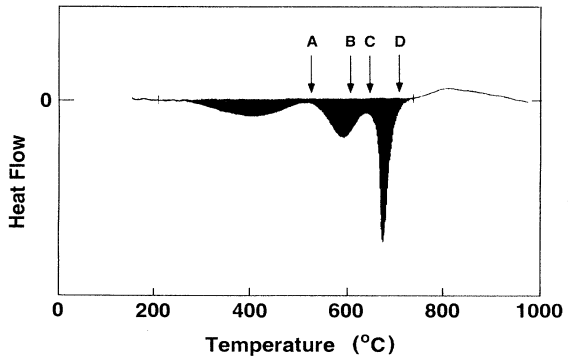

FIG. 4. DSC trace of a bcc $Ti_{60}Cr_{40}$ alloy, heated with a rate of 20 K/min. The arrows indicate the temperatures up to which additional runs were performed in order to characterize the corresponding structural changes.

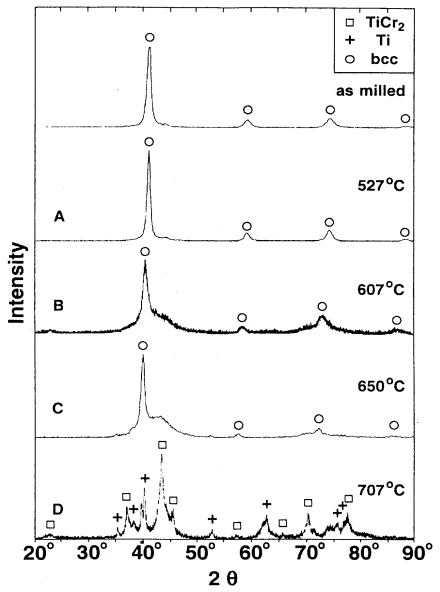

FIG. 5. X-ray-diffraction patterns of bcc $Ti_{60}Cr_{40}$ heated to the temperatures indicated in Fig. 4.

crystallization. The Williamson and Hall analysis shows that the mean crystallite size and the rms strain have changed to 120 nm and 1.4%, respectively, indicating that the exothermic heat release up to about 500 °C originates mainly from the growth of the crystallites.

Upon further heating, the XRD pattern changes more drastically, and a diffuse diffraction halo at $2\Theta = 42°$ appears during the second exothermic peak at around 580 °C. The bcc diffraction intensities decrease and the peaks shift to lower angles. The position and the width of the diffraction halo are in good agreement with results for amorphous TiCr alloys prepared by co-sputtering of the elemental components, the structure of which has been confirmed by TEM observations.[24] The concentration of the remaining bcc phase is determined to be 23 at. % Cr according to Eq. (1). Therefore, during the second exothermic reaction, a Cr-richer amorphous phase precipitates from the $Ti_{60}Cr_{40}$ alloy, resulting in a decrease of the Cr content in the bcc parent phase. This reaction overlaps slightly with the formation of the equilibrium phases, hcp Ti and $TiCr_2$, as the results obtained after heating to 650 °C indicate. Thermodynamic equilibrium is reached by annealing above 700 °C. The corresponding exothermic peak in the DSC scan at $T = 680$ °C therefore mainly originates from the crystallization of the amorphous phase. It should be mentioned that no difference in the phase formation was obtained whether the thermal treatment was performed in pure argon or nitrogen in a DSC cell, or pure nitrogen, argon, or vacuum in a quartz tube.

In addition, isothermal annealing at 550 °C was made in the DSC for different times, and the structural evolution was characterized by XRD as shown in Fig. 6. It demonstrates that an amorphous phase has been formed after 20 min at the expense of the bcc phase, which again exhibits a Ti-richer concentration with respect to the ini-

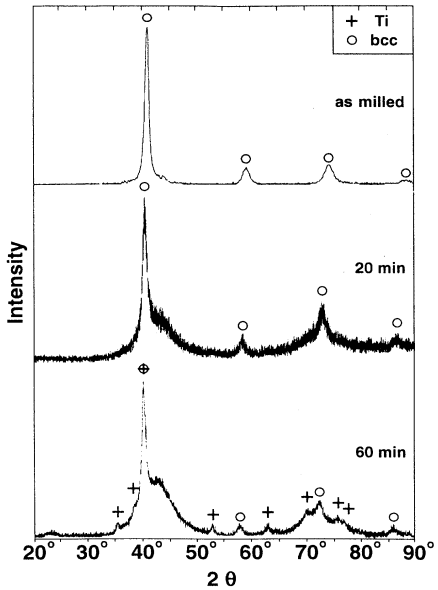

FIG. 6. X-ray-diffraction patterns of a bcc $Ti_{60}Cr_{40}$ alloy after isothermal heating at 550 °C for different times.

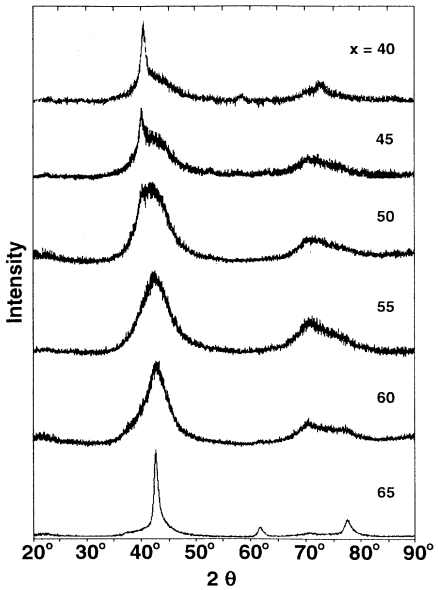

FIG. 7. X-ray-diffraction patterns of $Ti_{100-x}Cr_x$ as a function of Cr content, annealed up to the end of the second exothermic peak in the DSC.

tial composition, and that traces of hcp Ti could be already detected after 60 min. Isothermal annealing at 600 °C for 24 h has led to complete transformation into the equilibrium phases hcp Ti and $TiCr_2$, in agreement with Refs. 10, 11, and 13, but in contrast to Ref. 6, where an amorphization was observed.

In principle the results reported above support the claimed amorphization of bcc $Ti_{60}Cr_{40}$ alloys by Blatter and von Allmen,[5,6] but differ in two aspects: first, amorphization is associated with a decomposition rather than with a polymorphous transition; second, the amorphous phase forms at a lower temperature or shorter annealing time. With respect to the first point, the formation of a Cr-richer amorphous phase indicates that complete amorphization or inverse melting can be expected only in a bcc phase with more than 40 at. % Cr. Lower Cr contents seem to be unfavorable for inverse melting in contrast to the results reported in Ref. 5. The different preparation method may be considered as a main reason for the second point, because the very fine-grained bcc phase produced by mechanical alloying may favor amorphization by providing a high density of heterogeneous nucleation sites. Grain boundaries were reported to play a key role in the nucleation of an amorphous phase during solid-state reactions of NiZr (Ref. 25) and Fe-Zr,[26] as well as for the precipitation of an amorphous phase from a solid solution.[27]

C. Concentration dependence of the amorphization

Figure 7 represents, as a function of Cr content, the XRD patterns for samples heated up to the end of the amorphization reaction as deduced from the DSC signal. It is shown that complete amorphization is achieved only for a bcc $Ti_{45}Cr_{55}$ alloy, while partial amorphization is observed for other compositions. The first diffraction halos of amorphous $Ti_{50}Cr_{50}$ and $Ti_{45}Cr_{55}$ alloys are at $2\Theta = 41.73°$ and 42.47°, respectively, which are comparable with the results for amorphous TiCr alloys prepared by sputtering.[24]

Figures 8 and 9, respectively, show TEM micrographs for a $Ti_{50}Cr_{50}$ sample before and after annealing for 30 min at 577 °C. The as-milled powder exhibits a bcc structure with crystallite sizes in the range from 10–30 nm. However, as already suggested by the XRD pattern (cf. Fig. 2) some Cr-rich crystallites can be determined by energy-dispersive x-ray (EDX) analyses with a 10-nm probe. After annealing, the diffuse diffraction halos and the lack of image contrast confirm the formation of an amorphous phase (Fig. 9). The few crystallites still visible in the amorphous matrix exhibit a Cr-rich composition and are obviously related to the Cr-rich areas already observed in the as-milled sample which may give rise to the asymmetry of the second diffuse diffraction maximum of the amorphous phase (Fig. 7). This result indicates that complete amorphization can only be obtained if the initial bcc alloy is homogeneous on a nanometer scale, which requires special milling conditions during mechanical alloying. However, with respect to the conclusions given in this paper, the small volume fractions of the Cr-rich crystallites can be neglected.

Figure 10 shows for $Ti_{60}Cr_{40}$, $Ti_{45}Cr_{55}$, and $Ti_{35}Cr_{65}$ alloys the development of the (110) peaks for parent bcc alloys upon annealing. In the case of $Ti_{45}Cr_{55}$, the amorphous phase forms at the expense of the bcc phase which exhibits a constant (110) peak position during annealing, while for $Ti_{60}Cr_{40}$ and $Ti_{35}Cr_{65}$ alloys the (110) peak shifts to lower and higher diffraction angles, respectively. This demonstrates that the complete amorphization observed for 55 at. % Cr is indeed a polymorphous transition, while a decomposition occurs for other concentrations. Furthermore, the results shown in Figs. 7 and 10 strongly

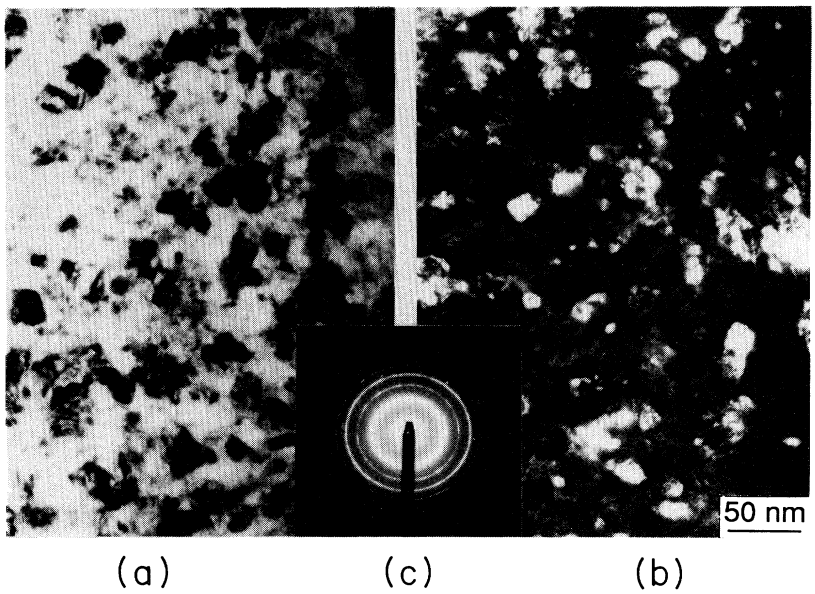

FIG. 8. TEM micrographs of $Ti_{50}Cr_{50}$ after mechanical alloying for 100 h. (a) bright field image, (b) dark field image, $\vec{g}=(110)$, (c) corresponding selected area diffraction pattern.

imply that in the final annealing state the amorphous phase is in a metastable equilibrium with the bcc phase. We will discuss this point later by means of the CALPHAD method.

D. Kinetics of phase transformations

The structural changes upon annealing observed for the bcc $Ti_{60}Cr_{40}$ alloy demonstrate the kinetic competition between the amorphization and the formation of the equilibrium phases. For heat treatments at low temperatures and with Cr contents up to 50 at. %, the precipitation of the hcp Ti-rich phase limits the amorphization reaction, whereas at higher temperatures crystallization of the amorphous phase into $TiCr_2$ accompanies the nucleation of the hcp phase. For Cr concentrations between 55 and 65 at. %, $TiCr_2$ is the first equilibrium phase observed upon annealing. This finding can be understood from the phase diagram by considering a metastable ex-

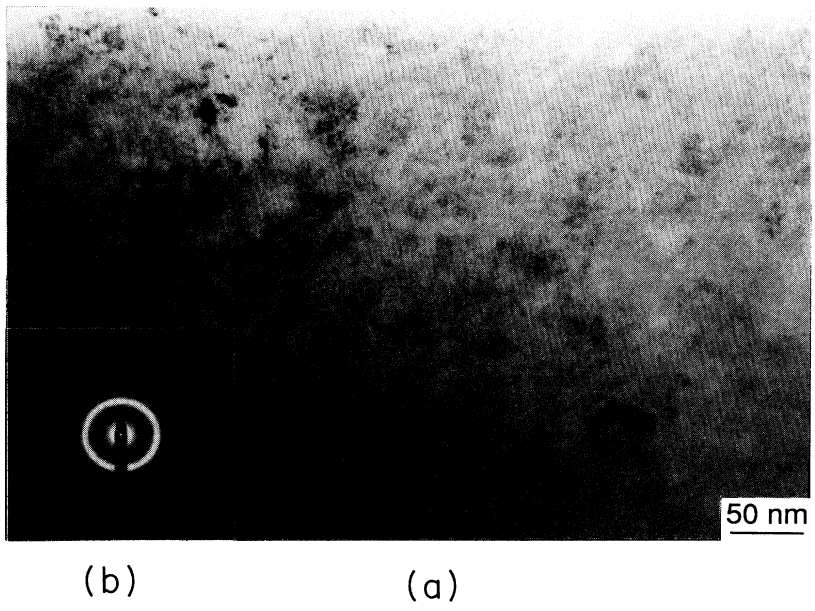

FIG. 9. TEM bright field micrograph (a) and diffraction pattern (b) of $Ti_{50}Cr_{50}$ after mechanical alloying for 100 h and annealing at 577 °C for 30 min.

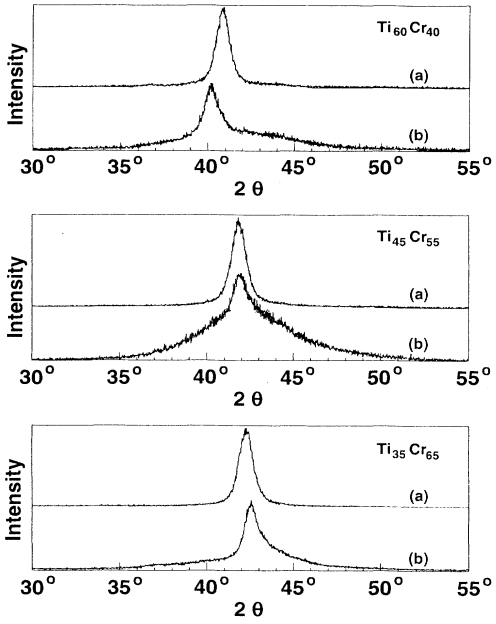

FIG. 10. Evolution of the (110) Bragg peak of the bcc phase (a) for the as-milled state and (b) during amorphization for different Cr concentrations.

tension of the homogeneity range of the Laves phase.

In order to obtain a time-temperature-transformation diagram, the annealing behavior for a bcc $Ti_{55}Cr_{45}$ alloy has been studied in detail. Samples were heated up in the DSC for different heating rates ranging from 5 to 160 K/min, and the onset temperatures for amorphization and for crystallization were determined from the beginning of the corresponding exothermic heat releases. The results are summarized in Fig. 11 and show that slow heating rates or long annealing times at low temperatures favor amorphization. This conclusion is further supported by considering the activation enthalpies of the amorphization and of the crystallization, which have been derived from the DSC measurements by applying the Kissinger method.[28] Thereby the activation enthalpies are determined from the slope of $\ln(\dot{T}/T_m^2)$ versus $\ln(1/T_m)$, where $\dot{T}$ is the heating rate and T_m the peak temperature of the exothermic heat release. The activation enthalpies thus obtained amount to 2.3 eV for amorphization and 3.2 eV for crystallization. Kim and Lee[9] reported corresponding values of 2 and 2.7 eV, respectively, for a bcc $Ti_{60}Cr_{40}$ alloy, which are slightly lower than those we obtained for $Ti_{55}Cr_{45}$.

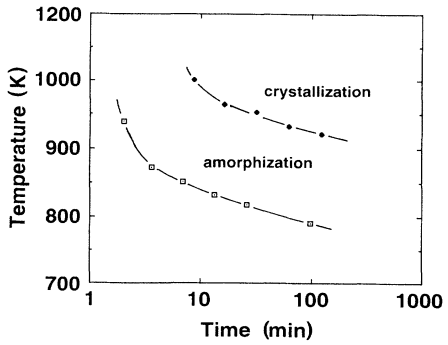

FIG. 11. Time-temperature-transformation diagram for the phase transformations occurring in bcc $Ti_{55}Cr_{45}$. The data points represent the onset temperatures of amorphization (□) and subsequent crystallization (♦) as obtained from DSC scans by applying different heating rates.

TABLE I. Activation enthalpies (eV/atom).

at. % Cr	0	10	18	40	45
Diffusion of Cr in bcc alloys	1.64[a]	1.74[a]	1.93[a]		
Amorphization of bcc alloys				2.0[b]	2.3[c]

[a]Reference 29.
[b]Reference 9.
[c]This work.

The activation enthalpies for the amorphization agree reasonably with the activation enthalpies of Cr diffusion in bcc TiCr alloys which have been determined for concentrations up to 18 at. % Cr (Ref. 29) (Table I). This suggests that the formation of the amorphous phase is determined by the fast diffusing Cr component in the bcc alloy. The high activation energy of about 3 eV for the formation of the equilibrium phases may be due to a high interface enthalpy required for nucleation, and due to the high activation enthalpy for the Ti diffusion required for transformation into the stable phases. Similar kinetic arguments have been given to describe the preferred formation of the amorphous phase with respect to the intermetallic compounds in thin-film diffusion couples.[1] We therefore conclude that inverse melting can only be observed if a difference in the activation enthalpies for amorphization and for the formation of the equilibrium phases exists, and that this is most likely in systems in which the components exhibit large differences in diffusivity.

IV. DISCUSSION

The experimental results show a polymorphous transformation of the bcc alloy into an amorphous phase for a Cr content of 55 at. %. This indicates that, at temperatures of about 600 °C, a thermodynamic driving force must exist for the amorphization such that the free energy of the amorphous phase is lower than that of the bcc alloy for this particular concentration. This conclusion is confirmed by calculation of the thermodynamic functions in the Ti-Cr system utilizing the CALPHAD method. The calculations are based on the equilibrium phase diagram, available thermodynamic data from the literature,[22] and the heats of transformation upon annealing metastable bcc alloys as measured by DSC.[18] Details of the calculations and a discussion of the thermodynamics in the Ti-Cr system will be given in a forthcoming paper.

Figure 12 represents the free energy of the hcp, bcc, and the amorphous phases, at a temperature of 600 °C. The results clearly demonstrate the existence of a driving

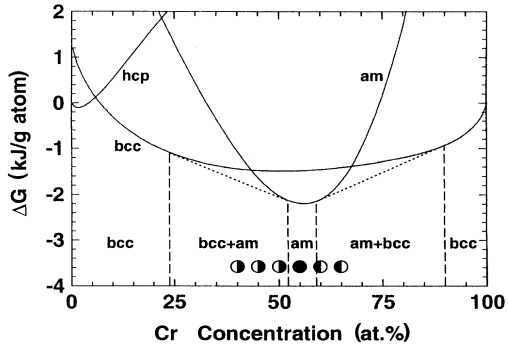

FIG. 12. Free-energy functions at $T = 600\,^{\circ}C$ of bcc, hcp, and amorphous phases in the Ti-Cr system, calculated by the CALPHAD method. The circles represent the experimental observations. ●: complete amorphization; ◑: amorphous phase coexisting with a Ti-rich β phase; ◐: amorphous phase coexisting with a Cr-rich β phase.

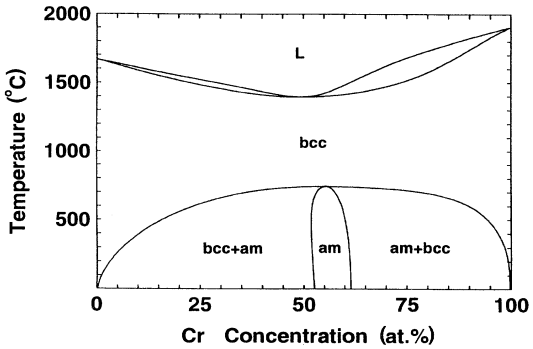

FIG. 13. Metastable phase diagram of the Ti-Cr system calculated by the CALPHAD method by considering only equilibria between the bcc alloy and the amorphous or the liquid phase.

force for the amorphization of the bcc alloy for compositions around 55 at. % Cr. However, the driving force amounts to only about 0.7 kJ/g-at. which is relatively small, if compared to other systems exhibiting a precipitation reaction of the amorphous phase (e.g., Nb-Co, Ref. 30). This indicates a possible nucleation barrier for the amorphization in the Ti-Cr system, which can be decreased by introducing a high density of heterogeneous nucleation sites such as grain boundaries and other defects, as already suggested in Ref. 23. It is believed that the microstructure obtained by mechanical alloying is kinetically favorable for the amorphization of bcc TiCr alloys due to the small crystallite size and the high dislocation density.

By applying the common-tangent rule, metastable equilibria between the amorphous and the bcc phase can be determined. At $T = 600\,^{\circ}C$ it results in a homogeneity range of the amorphous phase from 52 to 59 at. % Cr placed between two-phase fields which consist of the amorphous phase and a Ti-rich or Cr-rich bcc phase with 23 and 90 at. % respectively. In Fig. 12 these predictions are compared to the experimental observations, indicating that indeed metastable equilibria are obtained.

If the metastable equilibria between the bcc and the amorphous (at low temperatures) or the liquid phase (at high temperatures) are determined over the entire temperature range of coexistence, the metastable phase diagram can be derived (Fig. 13). It excludes the formation of the equilibrium hcp and Laves phases, which is reasonable in particular for low temperatures due to the kinetic constraints determining the nucleation and growth of these phases. The metastable phase diagram predicts a congruent inverse melting point, T_{im} at about $746 \pm 20\,^{\circ}C$ and 55 at. % Cr. The thermodynamic functions for this composition show that, similar to other systems with negative heats of mixing,[16,17] the liquid develops short-range order upon undercooling, leading to a stabilization with respect to the crystalline phases. Thereby, the entropy as well as the enthalpy of the liquid is decreased below those of the bcc phase, which facilitates the inverse melting of the bcc phase. It is the advantage of the Ti-Cr system that the thermodynamics allow the inverse melting to occur at temperatures high enough where phase transformations are still kinetically possible.

From the thermodynamic point of view, the phase transition at the inverse melting point should be reversible. Upon heating above T_{im}, the amorphous phase should transform back into the bcc phase (which can be named correspondingly "inverse freezing"). Such behavior was claimed for $Ti_{70}Cr_{30}$ alloys.[5] However, from the results of our investigations this is thermodynamically impossible for the cited experimental conditions. Instead, it is suggested from Fig. 13 that annealing a bcc $Ti_{70}Cr_{30}$ alloy at $600\,^{\circ}C$ should result in the formation of a two-phase mixture of a Ti-rich bcc and an amorphous phase, the latter being dissolved into the bcc matrix upon heating to $800\,^{\circ}C$. A polymorphous reversible transition is thermodynamically possible only for Cr concentrations around 55 at. %. However, by heating an amorphous $Ti_{45}Cr_{55}$ alloy in a vacuum chamber, the *in situ* x-ray analysis shows that the equilibrium phases are formed prior to the transformation into the bcc phase. This is in agreement with DSC results, which show no (endothermic) crystallization of the amorphous phase into the bcc phase below the temperature where nucleation of the $TiCr_2$ compound occurs. These results demonstrate that the direct observation of the reversibility of the inverse melting transition is limited by the formation of the equilibrium phases.

V. CONCLUSIONS

In the Ti-Cr system, a polymorphous transformation of the metastable bcc phase into an amorphous phase is observed for a Cr content of 55 at. %. For other compositions the amorphous phase coexists with a Ti-rich or Cr-rich bcc phase after annealing. These results can be described by the metastable phase diagram calculated by the CALPHAD method which considers only equilibria between the bcc alloy and the amorphous or liquid phase. It indicates that inverse melting in the Ti-Cr system is thermodynamically possible only for compositions around 55 at. % Cr, in contrast to earlier reports.[5,6] The

occurrence of inverse melting originates from a pronounced short-range ordering of the liquid upon undercooling, which stabilizes the liquid phase with respect to the bcc alloy.

Inverse melting can only be observed experimentally if the kinetics below the inverse melting point are sufficiently rapid to enable the phase transformation to occur, and if the amorphization is kinetically favored with respect to the formation of the equilibrium phases. The latter requirement is associated with different activation enthalpies for the competing processes, which is expected in particular in systems exhibiting fast diffusion of one component. However, due to the high inverse melting temperature of about 750 °C for bcc Ti-Cr alloys, the reversibility of the polymorphous transition between the amorphous and the bcc phase could not be confirmed experimentally yet.

ACKNOWLEDGMENTS

We thank P. A. Beaven and S. Wöhlert for valuable discussions and experimental help, and F. Schmelzer for chemical analyses. The financial support of the Deutsche Forschungsgemeinschaft (Leibniz-Programm) is also gratefully acknowledged.

*Present address: Institut de Recherche d'Hydro-Québec, Varennes, Québec, Canada J3X 1S1.

[1]W. L. Johnson, Prog. Mater. Sci. **30**, 81 (1986).
[2]R. B. Schwarz and W. L. Johnson, Phys. Rev. Lett. **51**, 415 (1983).
[3]C. C. Koch, O. B. Cavin, C. G. Mc Kamey, and J. O. Scarbrough, Appl. Phys. Lett. **43**, 1017 (1983).
[4]E. G. Ponyatovsky, I. T. Belash, and O. I. Barkalov, J. Non-Cryst. Solids. **117/118**, 679 (1990).
[5]A. Blatter and M. von Allmen, Phys. Rev. Lett. **54**, 2103 (1985).
[6]A. Blatter, M. von Allmen, and N. Baltzer, J. Appl. Phys. **62**, 276 (1987).
[7]A. L. Greer, J. Less-Common Met. **140**, 327 (1988).
[8]R. Bormann, Habilitation-thesis, Göttingen, 1988.
[9]Y.-G. Kim and J.-Y. Lee, J. Non-Cryst. Solids **122**, 269 (1990).
[10]R. Prasad, R. E. Somekh, and A. L. Greer, Mater. Sci. Eng. **A133**, 606 (1991).
[11]W. Sinkler and D. E. Luzzi, in *Kinetics of Phase Transformations,* edited by M. O. Thompson, M. Aziz, and G. B. Stephenson, MRS Symposia Proceedings No. 205 (Materials Research Society, Pittsburgh, 1991), p. 204.
[12]L. J. Gallego, J. A. Somoza, and J. A. Alonso, Physica B **160**, 108 (1989).
[13]K. Ohsaka, E. H. Trinh, J. C. Holzer, and W. L. Johnson, Appl. Phys. Lett. **60**, 1079 (1992).
[14]M. Oehring, Z. H. Yan, T. Klassen, and R. Bormann, Phys. Status Solidi A **131**, 671 (1992).
[15]H. L. Lukas, J. Weiss, and E. T. Henig, CALPHAD **6**, 229 (1982).
[16]R. Bormann, F. Gärtner, and K. Zöltzer, J. Less-Common Met. **145**, 19 (1988).
[17]R. Bormann and K. Zöltzer, Phys. Status Solidi A **131**, 691 (1992).
[18]W. Poeβnecker, G. Leitner, M. Oehring, and R. Bormann (unpublished).
[19]M. J. Blackburn and J. C. Williams, Trans. Amer. Inst. Met. **239**, 287 (1967).
[20]G. K. Williamson and W. H. Hall, Acta Metall. **1**, 22 (1953).
[21]Z. H. Yan, M. Oehring, and R. Bormann, J. Appl. Phys. **72**, 2478 (1992).
[22]J. L. Murray, Bull. Alloy Phase Diag. **2**, 174 (1981).
[23]A. Blatter, U. Kambli, Ch. Wirz, R. Giovanoli, K. Dyrbye, and J. Bøttiger, Phys. Rev. B **40**, 12 503 (1989).
[24]C. Michaelsen, Z. H. Yan, and R. Bormann, J. Appl. Phys. **73**, 2249 (1993).
[25]W. J. Meng, C. W. Nieh, E. Ma, B. Fultz, and W. L. Johnson, Mater. Sci. Eng. **97**, 87 (1988).
[26]W. Kiauka, C. Van Cuyck, and W. Keune, Mater. Sci. Eng. B **12**, 273 (1992).
[27]W. Biegel, W. Schaper, H.-U. Krebs, J. Hoffmann, H. C. Freyhardt, R. Busch, and R. Bormann, J. Phys. (Paris), Colloq. **51**, C4-189 (1990).
[28]H. E. Kissinger, Anal. Chem. **29**, 1702 (1957).
[29]A. J. Mortlock and D. H. Tomlin, Philos. Mag. **4**, 628 (1959).
[30]R. Bormann and R. Busch, J. Non-Cryst. Solids **117/118**, 539 (1990).

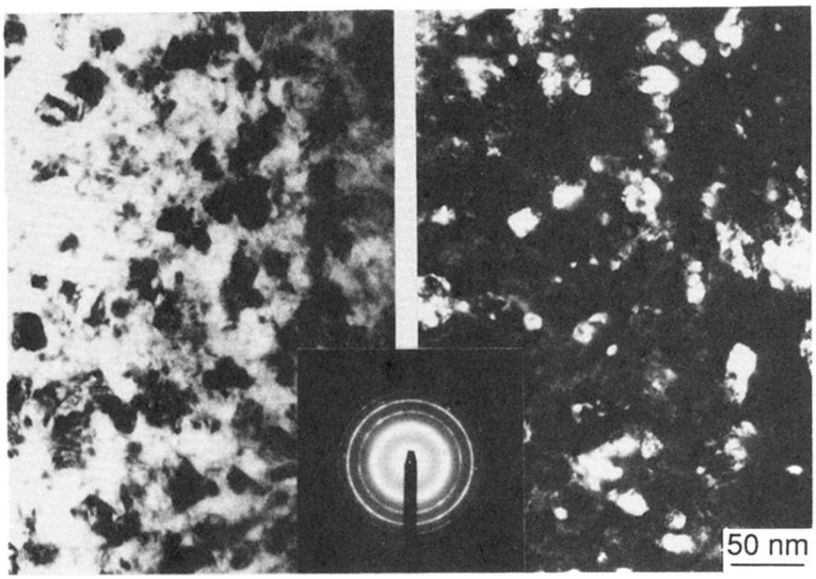

FIG. 8. TEM micrographs of $Ti_{50}Cr_{50}$ after mechanical alloying for 100 h. (a) bright field image, (b) dark field image, $\vec{g}=(110)$, (c) corresponding selected area diffraction pattern.

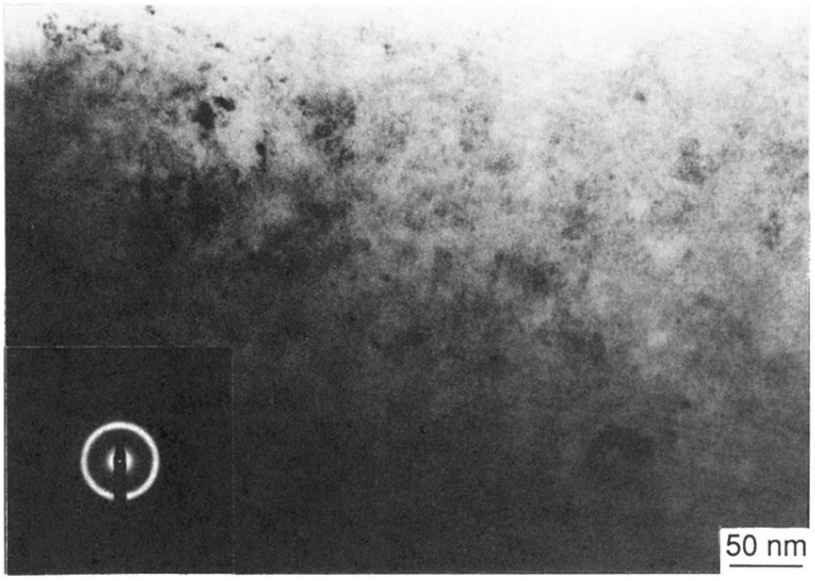

FIG. 9. TEM bright field micrograph (a) and diffraction pattern (b) of $Ti_{50}Cr_{50}$ after mechanical alloying for 100 h and annealing at 577 °C for 30 min.